

## REFLECT – Research flight of EURADOS and CRREAT: Intercomparison of various radiation dosimeters onboard aircraft

Iva Ambrožová<sup>a,\*</sup>, Peter Beck<sup>b</sup>, Eric R. Benton<sup>a,c</sup>, Robert Billnert<sup>d</sup>, Jean-Francois Bottollier-Depois<sup>e</sup>, Marco Caresana<sup>f</sup>, Nesrine Dinar<sup>g</sup>, Szymon Domański<sup>h</sup>, Michał A. Gryziński<sup>h</sup>, Martin Kákona<sup>a,i</sup>, Antonín Kolros<sup>j,k</sup>, Pavel Krist<sup>a</sup>, Michał Kuć<sup>h</sup>, Dagmar Kyselová<sup>a,i</sup>, Marcin Latocha<sup>b</sup>, Albrecht Leuschner<sup>l</sup>, Jan Lillhök<sup>d</sup>, Maciej Maciak<sup>h</sup>, Vladimír Mareš<sup>m</sup>, Łukasz Murawski<sup>h</sup>, Fabio Pozzi<sup>g</sup>, Guenther Reitz<sup>a,n</sup>, Kai Schennetten<sup>n</sup>, Marco Silari<sup>g</sup>, Jakub Šlegl<sup>a,i</sup>, Marek Sommer<sup>a,i</sup>, Václav Štěpán<sup>a</sup>, Francois Trompier<sup>e</sup>, Christoph Tscherne<sup>b</sup>, Yukio Uchihori<sup>o</sup>, Arturo Vargas<sup>p</sup>, Ladislav Viererbl<sup>j,k</sup>, Marek Wielunski<sup>m</sup>, Mie Wising<sup>d</sup>, Gabriele Zorloni<sup>f</sup>, Ondřej Ploc<sup>a</sup>

<sup>a</sup> Nuclear Physics Institute CAS, Czech Republic

<sup>b</sup> Seibersdorf Labor GmbH, Austria

<sup>c</sup> Oklahoma State University, USA

<sup>d</sup> Swedish Radiation Safety Authority, Sweden

<sup>e</sup> Institute for Radiological Protection and Nuclear Safety, France

<sup>f</sup> Politecnico di Milano, Italy

<sup>g</sup> CERN, Switzerland

<sup>h</sup> National Centre for Nuclear Research, Poland

<sup>i</sup> Faculty of Nuclear Sciences and Physical Engineering CTU, Prague, Czech Republic

<sup>j</sup> Research Centre Rez, Czech Republic

<sup>k</sup> HHtec Association, Czech Republic

<sup>l</sup> Deutsches Elektronen-Synchrotron, Germany

<sup>m</sup> Helmholtz Zentrum München, Germany

<sup>n</sup> German Aerospace Center, Germany

<sup>o</sup> National Institute of Radiological Sciences / QST, Japan

<sup>p</sup> Technical University of Catalonia, Spain

### ARTICLE INFO

#### Keywords:

Cosmic radiation  
Aircraft  
Dosimeter  
Intercomparison  
Research flight

### ABSTRACT

Aircraft crew are one of the groups of radiation workers which receive the highest annual exposure to ionizing radiation. Validation of computer codes used routinely for calculation of the exposure due to cosmic radiation and the observation of nonpredictable changes in the level of the exposure due to solar energetic particles, requires continuous measurements onboard aircraft. Appropriate calibration of suitable instruments is crucial, however, for the very complex atmospheric radiation field there is no single reference field covering all particles and energies involved. Further intercomparisons of measurements of different instruments under real flight conditions are therefore indispensable.

In November 2017, the REFLECT (**RE**search **FL**ight of **EUR**ADOS and **CR**REAT) was carried out. With a payload comprising more than 20 different instruments, REFLECT represents the largest campaign of this type ever performed. The instruments flown included those already proven for routine dosimetry onboard aircraft such as the Liulin Si-diode spectrometer and tissue equivalent proportional counters, as well as newly developed detectors and instruments with the potential to be used for onboard aircraft measurements in the future. This flight enabled acquisition of dosimetric data under well-defined conditions onboard aircraft and comparison of new instruments with those routinely used.

As expected, dosimeters routinely used for onboard aircraft dosimetry and for verification of calculated doses such as a tissue equivalent proportional counter or a silicon detector device like Liulin agreed reasonable with

\* Corresponding author. Nuclear Physics Institute CAS, Department of Radiation Dosimetry, Na Truhlárce 39/64, Prague, 18000, Czech Republic.

E-mail address: [ambrozova@ujf.cas.cz](mailto:ambrozova@ujf.cas.cz) (I. Ambrožová).

<https://doi.org/10.1016/j.radmeas.2020.106433>

Received 9 March 2020; Received in revised form 8 July 2020; Accepted 9 July 2020

Available online 23 July 2020

1350-4487/© 2020 The Authors.

Published by Elsevier Ltd.

This is an open access article under the CC BY-NC-ND license

(<http://creativecommons.org/licenses/by-nc-nd/4.0/>).

each other as well as with model calculations. Conventional neutron rem counters underestimated neutron ambient dose equivalent, while extended-range neutron rem counters provided results comparable to routinely used instruments. Although the responses of some instruments, not primarily intended for the use in a very complex mixed radiation field such as onboard aircraft, were as somehow expected to be different, the verification of their suitability was one of the objectives of the REFLECT. This campaign comprised a single short flight. For further testing of instruments, additional flights as well as comparison at appropriate reference fields are envisaged. The REFLECT provided valuable experience and feedback for validation of calculated aviation doses.

## 1. Introduction

Aircraft crew and airline passengers are exposed to elevated dose rates due to cosmic radiation onboard aircraft; aircraft crew is considered as a group of workers receiving one of the highest annual effective doses (ICRP, 1991; ICRP, 2007; ICRP, 2016; IAEA, 2003). Radiation protection for aircraft crew has been regulated in the European Union since 1996 by the EU-Directive 29/96/EURATOM (EURATOM, 1996). Since then, this directive was updated with the EU-Directive 2013/59/EURATOM (EURATOM, 2013). The EU member states were obliged to comply with the new regulations by updating their national legislations by February 2018. Annual personal doses from galactic cosmic radiation (GCR) to aircraft crew members are routinely calculated by various computer codes that are validated preferably by measurements but also by code intercomparisons. Ongoing validations of such codes need in-flight measurements with appropriately calibrated instruments.

An assessment of aircraft crew radiation exposure is a complex task. Radiation field at civil flight altitudes is formed by interactions of mainly GCR (and sporadically solar energetic particles – SEP) with the atoms of the atmosphere of the Earth. All types of particles and electromagnetic component such as protons, muons, pions, electrons, neutrons, gamma rays and others of a wide range of energies covering several orders of magnitude are present as primary or secondary radiation (Schraube et al., 2000; ISO, 2001; Lindborg et al., 2004). Depending on altitude and geomagnetic latitude, about 40%–70% of ambient dose equivalent  $H^*(10)$  is due to neutrons, 20%–30% due to electrons, 10% due to protons and 10% due to photons and muons (Schraube et al., 2002a; Lindborg et al., 2004). In addition, radiation field in the atmosphere is not constant in time and space due to solar modulation of the GCR, strong variations of particle fluences and energies in occasional SEPs, latitude effects caused by the geomagnetic field and build-up/absorption effects resulting from nuclear reactions with the atmospheric nuclei.

An assessment of the radiation exposure of aircraft crew requires a determination of the radiation protection quantity effective dose  $E$  (ICRP, 2007). Since the effective dose is not a measurable quantity, for operational radiation protection purposes, an operational quantity, the ambient dose equivalent  $H^*(10)$  was introduced (ICRU, 1993).  $H^*(10)$  should be a conservative estimate of  $E$ . An empirical determination of  $H^*(10)$  onboard aircraft requires accurate measurements using radiation detectors sensitive to the different particles and energy ranges. The most important species are neutrons (from few hundred keV up to few GeV) as they deliver the largest fraction of dose. The  $H^*(10)$  can be measured with an instrument suitably calibrated for this quantity what is not a trivial task for instruments to be used in atmospheric radiation field. For the very complex atmospheric radiation field, with its broad range of different particles and energies, there exists no single reference field covering all those radiation components. ISO reference radiation fields do not fully cover the whole particle and energy range of interest (ISO, 2012). Additionally, for proper calibration, instrument responses for all particles and energies shall be taken into account. To simulate a cosmic radiation field or some of its components at aviation altitude, an accelerator-produced field such as provided at CERN EU High Energy Reference Field (CERF) facility (Silari and Pozzi, 2017; Pozzi et al., 2017; Pozzi and Silari, 2019) or fields at high-mountains could be also

used. However, the composition and spectra of these fields are not exactly the same as the one present onboard aircraft. Today, well calibrated Tissue Equivalent Proportional Counters (TEPC) are considered as the instruments that reasonably well approximate the operational dose quantity ambient dose equivalent in atmospheric radiation field (ISO, 2012, Lindborg et al., 1999). Other instruments need to be calibrated in appropriate reference fields or in situ against a TEPC.

Many in-flight measurements with different instruments were performed in the past and an overview of the most important research projects in aviation dosimetry during 1997–2007 was given in Beck (2009). Further descriptions and results from various measurement campaigns onboard aircraft between 1992 and 2003 have been summarized in Lindborg et al. (2004). Such measurements were usually done on single flights with changing altitude and cut-off rigidity (Bottollier-Depois et al., 2004; Kubančák et al., 2015). For constant flight conditions, measurements have been conducted with only a limited number of instruments, such as TEPC and silicon spectrometers (Meier et al., 2016; Lindborg et al., 2007; Latocha et al., 2007; Lillhök et al., 2007). Recently several new detectors that are potentially suitable for onboard aircraft dosimetry have been developed, but not yet fully tested in the field (Bottollier-Depois et al., 2019; Yasuda et al., 2020; Kákona et al., 2019).

Despite the measurements performed so far, there is still need for continuous measurements onboard aircraft especially for observing short-term variations of radiation levels associated with SEP. The silicon spectrometer Liulin has been used onboard aircraft for many years. Several Liulin detectors are permanently installed onboard aircraft of Air France and Czech airlines (Ploc et al., 2013) although their sensitivity to neutrons is rather low and they are not tissue-equivalent. A TEPC (e.g. like Hawk-type) is typically not used for long-term measurements due to its rather large dimensions and relatively high power consumption. A unique exception is long-term TEPC measurements reported by (Beck et al., 2005) where the “Halloween Storms” between October and November 2003 were recorded.

Intercomparisons with different types of instruments, which are usually calibrated in different ways, are necessary. A comparison exercise employing different instruments conducted in regular time intervals (e.g. every few years) represents an independent form of a quality control for participating groups. In addition, in a view of a growing demand for increasing the quality of dosimetric measurements at aviation altitudes by the space weather community (Tobiska et al., 2015; Meier et al., 2018) measurement campaigns onboard aircraft are necessary.

In November 2017, the research campaign REFLECT (REsearch FLight of EURADOS and CREAT) was carried out by Nuclear Physics Institute CAS. The response of more than 20 different detectors was investigated during a flight onboard a small aircraft. The instruments' ensemble included those already proved for dosimetry onboard aircraft such as Liulin and TEPCs, as well as newly developed detectors and instruments with the potential to be used for onboard aircraft measurements in future. Dosimetric data under well-defined conditions, including constant altitude and constant space weather conditions, were acquired. Sixteen institutes participated, several of them representing the leading research groups in aviation dosimetry in their respective countries. As a result, REFLECT is the largest campaign of this type ever

performed. This campaign was part of the research activities of Working Group 11 of EURADOS (EURADOS, 2020) and of the CRREAT (Research Center of Cosmic Rays and Radiation Events in the Atmosphere) project (CRREAT n.d.).

## 2. Instruments

Radiation detectors included in the REFLECT campaign embraced instruments routinely used for cosmic radiation monitoring (TEPC, Liulin), newly developed radiation detectors as well as detectors with future potential for cosmic radiation monitoring onboard aircraft. With one exception, all instruments were active radiation detectors, i.e. electronic instruments capable of making time-resolved measurements.

An overview of the detectors used listing instruments, measured quantities, typically used radiation fields and participating institutes is given in Table 1. The detectors routinely used are underlined. Others are various neutron rem-counters, Si-detectors, recombination chamber or scintillation detectors.

### 2.1. Tissue equivalent proportional counters (TEPC)

A TEPC has the ability to provide values of the dose equivalent in tissue-equivalent material from most radiation components reasonably well. It is therefore particularly useful in comparisons of cosmic radiation measurements onboard aircraft (EURADOS, 1996). Several different TEPCs were used to measure the dose equivalent during the REFLECT.

#### 2.1.1. Hawk environmental Monitoring System FW-AD

The Hawk environmental Monitoring System FW-AD is a tissue equivalent proportional counter from Far West Technology Inc. (Goleta, California, USA), composed of a spherical chamber (127 mm diameter) with a wall from A-150 tissue equivalent plastic (2 mm thick) and filled with pure propane gas at low pressure (about 9.33 hPa) simulating of 2  $\mu\text{m}$  site size (Conroy, 2004). The outer container is made of 6.35 mm thick stainless steel. The dose equivalent is calculated from a spectrum of single energy deposition events and a radiation quality factor  $Q$ , determined by the  $Q(L)$  relation given in ICRP 60 (ICRP, 1991), where  $L$  denotes the unrestricted linear energy transfer (LET) in the exposed material (ICRP, 2007).

Both IRSN and SL used Hawk type 1 systems using two linear multichannel analyzers working in parallel with low and high gains. The low-gain analogue to digital converter (ADC) measures LET spectra up to 1024  $\text{keV}\cdot\mu\text{m}^{-1}$  with 1  $\text{keV}\cdot\mu\text{m}^{-1}$  resolution. The high-gain channel uses an ADC measuring up to a lineal energy of 25.6  $\text{keV}\cdot\mu\text{m}^{-1}$  with a resolution of 0.1  $\text{keV}\cdot\mu\text{m}^{-1}$ . The energy deposition of the low-LET and high-LET components and the associated quality factor are stored in an output file once per minute. The separation between the low-LET and the high-LET component is set at 10  $\text{keV}\cdot\mu\text{m}^{-1}$  according to the  $Q(L)$  relationship (ICRP, 2007). Events, encountering significant electronic noise, below the so-called low energy threshold (0.3  $\text{keV}\cdot\mu\text{m}^{-1}$  for IRSN and 0.5  $\text{keV}\cdot\mu\text{m}^{-1}$  for SL) are not recorded. For the IRSN Hawk data analysis, a simple coefficient (the average of correction factor determined for  $^{60}\text{Co}$  and  $^{137}\text{Cs}$  gamma-rays) was applied (Farah et al., 2017). The same approach was taken for the SL Hawk. No compensation of the counting loss due to dead time is included in the analysis software.

Correction factors,  $N_{low}$  and  $N_{high}$  to ambient dose-equivalent for the low-LET and high-LET components of the dose equivalent are used.  $N_{low}$  was determined in photon radiation fields with  $^{60}\text{Co}$  and  $^{137}\text{Cs}$  sources.  $N_{high}$  was defined using the neutron reference sources of  $^{241}\text{Am}$ -Be or  $^{252}\text{Cf}$  neutron sources. The values of  $N_{low}$  are  $1.11 \pm 0.02$  and  $1.34 \pm 0.03$  and the values of  $N_{high}$  are  $0.80 \pm 0.09$  and  $0.84 \pm 0.10$  for IRSN and SL, respectively. Correction coefficients for neutrons were also evaluated for between 0.5 and 19 MeV and were found similar to Am-Be or  $^{252}\text{Cf}$  neutron sources (Trompier et al., 2007).

**Table 1**  
Instruments used during REFLECT.

| Instrument   | Quantity measured/<br>provided | Typical radiation field                                  | Institute   |
|--|--------------------------------|--|---|
| <u>TEPC Hawk</u>                                       | $H^*(10)$                      | Mixed radiation  | Institute for Radiological Protection and Nuclear Safety, France (IRSN) Seibersdorf Laboratories, Austria (SL)  |
| <u>Sievert instrument</u>                              | $H^*(10)$                      | Mixed radiation  | Swedish Radiation Safety Authority, Sweden (SSM)  |
| <u>Liulin</u>  | $D(\text{Si}), H^*(10)$        | Mixed radiation  | Nuclear Physics Institute of the CAS, Czech Republic (NPI) National Institute of Radiological Sciences, QST, Japan (QST) German Aerospace Center, Germany (DLR) |
| REM-2 recombination chamber                            | $H^*(10)$                      | Mixed radiation  | National Centre for Nuclear Research, Poland (NCBJ)   |
| LB 6419  | $H^*(10)$                      | Mixed radiation Neutrons (thermal – 300 MeV), photons    | Deutsches Elektronen-Synchrotron, Germany (DESY)  |
| TTM low-level neutron and gamma-ray monitoring station | $H^*(10)$                      | Mixed radiation  | National Centre for Nuclear Research, Poland (NCBJ)   |
| Airdos   | $D(\text{Si})$                 | Mixed radiation  | Nuclear Physics Institute of the CAS, Czech Republic (NPI)  |
| Minipix  | $D(\text{Si})$                 | Mixed radiation  | Nuclear Physics Institute of the CAS, Czech Republic (NPI)  |
| NM2B-495 Pb  | $H^*(10)$                      | Neutrons (up to 10 GeV)                                  | Helmholtz Zentrum München, Germany (HMGU)   |
| LINUS  | $H^*(10)$                      | Neutrons (up to 2 GeV)                                   | European Council for Nuclear Research, Switzerland (CERN)   |
| LB6411   | $H^*(10)$                      | Neutrons (up to 20 MeV)                                  | Nuclear Physics Institute of the CAS, Czech Republic (NPI)  |
| Passive REM counter                                    | $H^*(10)$                      | Neutrons   | Politecnico di Milano, Italy (Polimi)   |
| ELDO   | $H_p(10)$                      | Neutrons (up to 200 MeV)                                 | Helmholtz Zentrum München, Germany (HMGU)   |
| HammerHead HH  | $H^*(10)$                      | Photons (50 keV–8 MeV), electrons, protons, muons, pions | HHtec for HHtec Association, Czech Republic (HHtec)   |
| FH 40 G-10 with FHZ-612B probe                         | $H^*(10)$                      | Photons  | National Centre for Nuclear Research, Poland (NCBJ)   |

#### 2.1.2. Sievert instrument

The Sievert instruments are microdosimetric detectors developed by SSM (Kyllönen et al., 2001a; Lillhök et al., 2017). The detectors are TEPCs with 5 mm A-150 walls housed in vacuum containers of 2 mm aluminum. The detector volume has a diameter and length equal to 11.54 cm and a volume of 1207  $\text{cm}^3$ . The detectors are working at a gas pressure of 1.3 kPa of propane based tissue-equivalent gas with (volume fractions) 55%  $\text{C}_3\text{H}_8$ , 39.6%  $\text{CO}_2$  and 5.4%  $\text{N}_2$ , to simulate an object size with a mean chord length of 2  $\mu\text{m}$ .

The electric charge is integrated for an integration time of typically

0.1–0.3 s. The absorbed dose to detector gas during this time interval is calculated from the average charge, the mass of the detector gas, the mean energy required to create an ion pair (an average value of 27.2 eV was used in the analysis), and the detector gas multiplication factor.

Characterization of the radiation quality is based on the variance-covariance method (Kellerer, 1968; Bengtsson, 1970; Lindborg and Bengtsson, 1971; Kellerer and Rossi, 1984).

In cosmic radiation applications where the high-LET events are rare and the absorbed dose rate is relatively low, a mixed single-event and multiple-event analysis can be used (Kyllönen et al., 2001b). The measured spectrum will in such situations have a region dominated by multiple events, and another region dominated by single high-LET events. The regions are chosen to be separated at  $150 \text{ keV}\cdot\mu\text{m}^{-1}$ . The quality factor in the multiple-event region ( $<150 \text{ keV}\cdot\mu\text{m}^{-1}$ ) is calculated from the dose-average lineal energy by using a linear  $Q(y)$  relation. In the region above  $150 \text{ keV}\cdot\mu\text{m}^{-1}$ , the events are treated as single events (after correction for a multiple-event contribution),  $y$  was set equal to  $L$  and the corresponding absorbed dose fraction multiplied by the quality factor defined in ICRP 103 (ICRP, 2007). In addition, a correction factor  $c_{Q, \text{high}} = 1.25$  for the high-LET component below  $150 \text{ keV}\cdot\mu\text{m}^{-1}$  for the difference between the  $Q(y)$ -function used and  $Q(L)$  according to ICRP 60 (ICRP, 1991) is obtained from a previous comparison of the two approaches on aircraft measurements (Lillhök et al., 2007).

From Monte Carlo (MC) simulations of the neutron detector response (Lillhök, 2007) using a simulated atmospheric neutron spectrum (Roesler et al., 1998) the detector absorbed dose and the ambient absorbed dose  $D^*(10)$  agree within 3%.

The low-LET and high-LET components are defined as the contribution with dose-average lineal energy  $1.6 \text{ keV}\cdot\mu\text{m}^{-1}$  measured with these detectors in a  $^{60}\text{Co}$  gamma radiation field, and  $94 \text{ keV}\cdot\mu\text{m}^{-1}$  simulated for these detectors in a simulated atmospheric neutron spectrum (Lillhök, 2007).

## 2.2. Other detectors for mixed radiation fields

### 2.2.1. Liulin

The Mobile Dosimetry Unit (MDU) Liulin is a silicon semiconductor spectrometer that has been used for cosmic radiation measurements (Dachev, 2009) as well as aircraft crew dosimetry for many years (Ploc et al., 2013; Meier et al., 2009). Liulin is equipped with a Hamamatsu S2744-08 PIN diode ( $10 \times 20 \times 0.3 \text{ mm}^3$ ), low noise hybrid charge-sensitive preamplifier AMPTEK Inc. type A225, fast 12-bit analogue-digital converter (ADC), 2 or 3 microcontrollers and flash memory. Liulin detects energy imparted to its active volume in a single energy deposition event. Pulse amplitudes are stored in a 256-channel spectrum (only 8 most significant bits are used from ADC), from which the absorbed dose in silicon is then calculated. The energy calibration of Liulin was obtained at HIMAC (Uchihori et al., 2002).

Liulin can also be used to estimate  $H^*(10)$  onboard aircraft, using the absorbed dose in silicon and an appropriate conversion factor, which can be determined by various means (Ploc et al., 2011; Wissmann and Klages, 2018). In this experiment, several MDU models were used; however,  $H^*(10)$  is given only for Liulin MDU7 (NPI). MDU7 was recently calibrated at CERF, which enabled to obtain calibration coefficient converting  $D_{\text{Si}}$  to  $H^*(10)$  as described for example in Ploc et al. (2011).

### 2.2.2. Airdos

Airdos is detector with similar design and sensitivity as Liulin. It has been designed as open source instrument for measurement in mixed radiation fields with low intensity such as those encountered onboard aircraft (Kákona et al., 2019). It is composed of a silicon PIN diode (Hamamatsu S2744-09) of the same type used in the Liulin MDU, electronics for converting the signal to the pulse-height spectra, a GPS module, an SD memory card and batteries. Full documentation is freely

available at (GitHub, 2020). In this measurement campaign, a version Airdos 01 was used. Energy range of Airdos 01 is from 0.2 to 12.5 MeV of deposited energy in silicon with energy resolution 49.4 keV per channel. Accumulated pulse amplitudes are stored in 250 channels spectra every 15 s. The detector was calibrated using heavy charged particle beams at HIMAC (NIRS, Japan) and at the U-120M cyclotron (NPI, Czech Republic).

### 2.2.3. Timepix

Timepix (Llopert et al. 2002, 2007) is a hybrid semiconductor pixel detector which consists of matrix of  $256 \times 256$  pixels (total of 65536 pixels). Timepix was developed by Medipix2 collaboration (Campbell, 2011). The pixel pitch is  $55 \mu\text{m}$  and total sensitive area is nearly  $2 \text{ cm}^2$ . For this flight the silicon with thickness of  $500 \mu\text{m}$  was used as a semiconductor sensor chip. The Timepix chip was readout by compact electronics which is in MiniPIX interface (Granja et al., 2018; Granja and Pospisil, 2014). The detector was operated in per-pixel energy mode which allows to measure the time that the signal spent over threshold. The calibration between time over threshold to deposited energy was done by method described in (Jakubek, 2011). Due to high granularity provided by Timepix architecture the detector can measure single particle energy deposition events (Granja and Pospisil, 2014). The configuration of Timepix device and data acquisition (including the pre-processing of data) was performed in PIXET software (Turecek and Jakubek, 2015) which was run on standard Windows laptop.

### 2.2.4. REM-2 recombination chamber

The REM-2 is a cylindrical parallel-plate recombination chamber with an active volume of about  $1800 \text{ cm}^3$  and total mass of 6.5 kg. The chamber has 25 tissue-equivalent electrodes and it is filled with the gas mixture consisting of methane and 5% nitrogen, with high pressure up to 1 MPa. The effective wall thickness (Al) of the chamber is equivalent to about 1.8 cm of tissue. The REM-2 chamber approximates the dosimetric parameters of the ICRU sphere in such a way, that the dose contribution and energy spectrum of secondary charged particles in the chamber active cavity are similar to those in the ICRU sphere at the depth of 10 mm (Maciak, 2018). Therefore it can be used for the determination of  $H^*(10)$  in mixed radiation fields (Zielczyński et al., 2008; Caresana et al., 2014; Murawski et al., 2018).

The chamber is designed in such a way that the initial recombination of ions occurs when the chamber operates at polarizing voltages below saturation and, for a certain range of gas pressure and dose rates, the initial recombination exceeds volume recombination. Measuring methods are based on the determination of the dose rate from the saturation current and the radiation quality from the amount of initial recombination. By means of recombination methods it is possible to estimate the radiation quality factor (Zielczynski and Golnik, 1994; Golnik et al., 2004; Golnik, 2018).

The method used for the determination of the radiation quality involves measurements of two ionization currents  $i_S$  and  $i_R$  at two properly chosen polarizing voltages  $U_S$  and  $U_R$ . A certain combination of these two currents is called recombination index of radiation quality  $Q_4$  and may serve as a measurable quantity that depends on LET in a similar way as the radiation quality factor does (Golnik, 2018). The polarizing voltage  $U_S$  is the high voltage, the same as for the measurements of the absorbed dose. The lower voltage  $U_R$ , called the recombination voltage, has been determined during calibration of the chamber in a reference gamma radiation field of air kerma from  $^{137}\text{Cs}$  source.  $U_R$  ensures 96% of ion collection efficiency in such reference field. The ambient dose equivalent is calculated as the product of absorbed dose and  $Q_4$ .

The detector was calibrated at CERF in 2016, and twice in monoenergetic neutron reference fields: at PTB (Golnik et al., 1997) and in 2018 at NPL. Before the REFLECT measurements, the chamber was calibrated at 990 V saturation voltage in the accredited (AP 070) Radiation Protection Measurements Laboratory (LPD, NCBJ) according to the Operational procedure M-1 (2017) with a  $^{137}\text{Cs}$  reference photon

source and PuBe reference neutron source.

### 2.2.5. TTM low-level neutron and gamma-ray monitoring station

The low-level neutron and gamma-ray monitoring station registers photons and neutrons in separate ‘pulse-height’ windows (Pszona et al., 2014). The detector is based on an 8 inch Leake neutron area survey instrument (Leake, 2004). It uses a Centronic SP9  $^3\text{He}$  spherical proportional counter, surrounded by an inner polyethylene layer, a spherical shell of natural cadmium and a further outer polyethylene moderator. The cadmium shield is composed of two hemispherical shells, 0.91 mm thick, with 25 holes. The areas covered by the holes are the same in both hemispheres, except for a 12.5 mm hole used by the SP9 connector (Tagziria et al., 2004). Discrimination between photons and neutrons is based on the analysis of the pulse-height spectrum, defining the photon and neutron windows (Pszona et al., 2014). The neutron response function is shown in Fig. 1. The TTM station was calibrated with  $^{137}\text{Cs}$  and Am–Be reference sources in the accredited (AP 070) Radiation Protection Measurements Laboratory (LPD, NCBJ). Calibration factors used for the measurement were 0.55 nSv and 1.28 nSv per count for the photon and neutron windows, respectively.

### 2.2.6. LB 6419

The LB 6419 was designed by DESY and Berthold Technologies to measure the ambient dose equivalent  $H^*(10)$  of pulsed and continuous neutron and photon radiation at high-energy accelerators (Leuschner et al., 2017). The LB 6419 comprises a cylindrical moderated rem-counter with a  $^3\text{He}$  proportional counter and a plastic scintillator.

The response to low-energy neutrons  $H_{LEN}$  is obtained from the proportional counter by counting the reaction products of the nuclear reaction  $^3\text{He}(n,p)\text{T}$ . Its moderator is made of polyethylene and contains neither any response-shaping absorbers like Cd or B nor converters like Pb. So it measures  $H_{LEN}$  with a calibration factor of 0.1 nSv per count. Its neutron response function is shown in Fig. 1.

The response to high-energy neutrons  $H_{HEN}$  is obtained from the scintillator by collecting scintillator light above 20 MeV, a threshold where any response from electro-magnetic radiation such as  $\gamma$ ,  $e^\pm$ ,  $\mu^\pm$  can be discriminated. The response comes from the energy deposition of charged products from neutron scattering on hydrogen nuclei of the scintillator  $\text{H}(n,n)p$  and on carbon nuclei as  $\text{C}(n,p)$  and  $\text{C}(n,\alpha)$ . As this response is based on the measurement of absorbed energy rather than counting it cannot be shown in Fig. 1. The corresponding calibration

factor was measured and validated at CERF in 2010, 2012 and 2017.

The total neutron dose  $H_N$  is obtained by summing up the doses of the two energy ranges  $H_{LEN}$  and  $H_{HEN}$ .

Electromagnetic radiation ( $H_{ELM}$ ) can be separated from the neutron response because it shows up in the energy spectrum as the so called ‘muon peak’. In the cylindrical scintillator with its dimension of 4.1 cm these minimum ionizing particles lose about 8 MeV ( $2\text{ MeV}\cdot\text{cm}^{-2}$ ). The calibration is done by means of the Compton edges of radioactive sources such as  $^{137}\text{Cs}$  and  $^{60}\text{Co}$ .

Finally the total dose  $H_{TOT}$  is obtained by summing up the neutron dose  $H_N$  and the dose of the electro-magnetic radiation  $H_{ELM}$ .

### 2.2.7. HammerHead HH

The HammerHead HH (HHtec Association, Czech Republic) is a wide-range scintillation detector designed for high-precision  $H^*(10)$  measurements. The ambient dose equivalent rate range is from 5  $\text{nSv}\cdot\text{h}^{-1}$  to 10  $\text{mSv}\cdot\text{h}^{-1}$  for a photon energy range from 50 keV to 8 MeV. The typical type A uncertainty is 12% for 1 s measuring interval ( $1\sigma$  and  $H^*(10)_{\text{terrestrial}} = 130\text{ nSv}\cdot\text{h}^{-1}$ ). The HH meter is a portable detector with dimensions of  $\varnothing 80\text{ mm} \times 340\text{ mm}$  and mass of 1.6 kg.

The HammerHead HH has been designed in order that the measured value best corresponds to the physical definition of  $H^*(10)$  for photons and meet the strict criteria required by IEC 60846 for ambient dose equivalent meters. As detector, a  $\text{CaF}_2:\text{Eu}$  scintillator with low atomic number is used. Its shape is close to a sphere of 64 mm diameter, therefore the meter has excellent  $-135^\circ$  to  $+135^\circ$  angular response. The HH meter works in current mode, therefore the measurement is not influenced by dead time. The unique time-energy analysis of the measured signals makes it possible to distinguish the contribution  $H^*(10)_L$  from events with deposited energy below 4 MeV and  $H^*(10)_H$  from events with deposited energy above 4 MeV. When measuring on the Earth’s surface, the  $H^*(10)_L$  value represents the terrestrial component of the radiation field, whereas the  $H^*(10)_H$  value allows estimating the secondary cosmic ray component but without the influence of neutrons. The typical duration of a measurement is 9 h when the instrument is connected to a tablet for data transfer.

HammerHead HH was calibrated in the accredited calibration laboratory at Czech Metrology Institute in Prague with a X-ray device (40 keV–250 keV) and  $^{137}\text{Cs}$ ,  $^{60}\text{Co}$  reference sources in terms of  $H^*(10)$ .

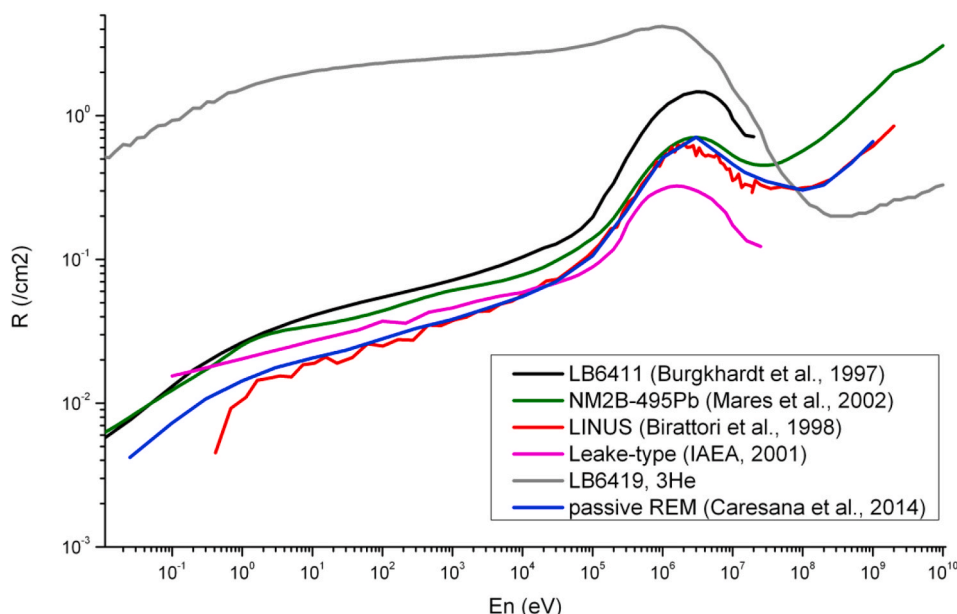


Fig. 1. Neutron response function  $R$  (counts per unit neutron fluence) of the neutron detectors used in REFLECT.

### 2.2.8. FH 40 G-10 with FHZ-612B probe

The FH 40 G-10 is a portable dose rate meter based on an internal energy filtered proportional counter. Without any external probe connected, this device is sensitive to photons only. During this experiment, an additional FHZ-612B Beta Gamma probe was connected. Even with the external FHZ-61B connected, the detector was used as gamma detector since the beta-ray detector cap was installed. The  $H^*(10)$  measuring ranges of the FH 40 G-10 and FHZ-612B are  $10 \text{ nSv}\cdot\text{h}^{-1} - 1 \text{ Sv}\cdot\text{h}^{-1}$  and  $100 \text{ nSv}\cdot\text{h}^{-1} - 10 \text{ Sv}\cdot\text{h}^{-1}$ , respectively. The energy range is 20 keV–4.4 MeV for the FH 40 G-10 and 82 keV–1.3 MeV for the FHZ-612B.

The instrument was calibrated in the accredited (AP 070) Radiation Protection Measurements Laboratory (LPD, NCBJ) with a  $^{137}\text{Cs}$  reference source in terms of  $H^*(10)$  (ISO, 1999).

## 2.3. Neutron rem-counters and dosimeters

Several neutron dosimeters and rem-counters were used. The design of neutron rem counters is based mostly on the Andersson-Braun type (Andersson and Braun, 1963) or Leake type (Leake, 1966) and they measure the neutron ambient dose equivalent,  $H^*(10)$ .

Neutron fluence response functions of the used neutron detectors are shown in Fig. 1. Response functions are usually calculated with MC codes; several energy points are validated through measurements in monoenergetic neutron fields.

### 2.3.1. NM2B–495 Pb rem counter

The NM2B–495 Pb Rem Counter is based on the conventional Andersson-Braun rem-counter (NE Technology Ltd.) with a cylindrical  $\text{BF}_3$  proportional counter surrounded by an inner polyethylene moderator, a boron-doped synthetic rubber absorber, and an outer polyethylene moderator. To extend the detection range to higher energy neutrons, a 1 cm thick lead shell is added around the boron rubber. For this experimental flight, pulse height spectra were registered to control the photon background and properly set up the region of interest (ROI). This procedure enables an appropriate evaluation of the number of counts which are then converted to  $H^*(10)$  through the calibration coefficient. The fluence response function from thermal to 10 GeV neutrons was calculated by means of different Monte Carlo codes (Mares et al., 2002). The rem counter calibration was performed using a 185 GBq  $^{241}\text{Am}$ –Be neutron source following the ISO recommendations (ISO, 2001). The rem counter was also used and calibrated in 100 and 300 MeV quasi-mono-energetic neutron fields at RCNP in Osaka (Mares et al., 2017) and at CERF. The response function of the detector is shown in Fig. 1.

### 2.3.2. LINUS

The LINUS (Birattari et al. 1990, 1992, 1993, 1998) is the original extended-range rem counter. It consists of a  $^3\text{He}$  proportional counter embedded in a spherical polyethylene moderator, which incorporates a boron-doped rubber absorber and a 1 cm thick lead shell so that its response function extends up to several hundred MeV. The signal is treated with a standard counting chain (pre-amplifier, amplifier, single channel analyzer and counter) and the TTL output is analyzed by a custom LabVIEW interface. The response function of the detector is shown in Fig. 1. Neutron detectors are sensitive to some extend to gamma rays, which can transfer energy to the system through Compton scattering in the walls or fill gas. The gamma rejection for the LINUS is obtained by setting a discriminator below the low energy neutron signal to reject counts due to gamma rays and electronic noise. The threshold was determined by analyzing the pulse height spectrum of the  $^3\text{He}$  counter.

The LINUS was calibrated with an Am–Be source (Dinar et al., 2017) in the CERN CALibration LABoratory (CALLAB) (Pozzi et al., 2015). The calibration provided a calibration factor of 0.89 nSv per count with an overall uncertainty of 3.2% at one sigma.

### 2.3.3. LB6411

The LB 6411 neutron probe (Burgkhardt et al., 1997), connected to the universal monitor LB 123, is designed for measurement of neutron ambient dose equivalent  $H^*(10)$  in accordance with ICRP 60 (BERTHOLD n.d.). The LB 6411 consists of a cylindrical  $^3\text{He}$  proportional counter centered in a polyethylene sphere with diameter 25 cm. The neutron energy range is from thermal to 20 MeV. The spectrum from the bare  $^{252}\text{Cf}$  neutron source has been used as the calibration spectrum. The numerical calibration factor is 0.32 nSv per count (Burgkhardt et al., 1997). The response function over the whole energy range was calculated with MCNP. For several energies the results were crosschecked with monoenergetic neutron measurements. The response function of the detector is shown in Fig. 1. The response to gamma radiation is approx.  $10^{-3}$  counts per nSv, which means a discrimination factor of  $3 \times 10^3$ .

### 2.3.4. Passive REM counter

The neutron contribution to  $H^*(10)$  was also measured with a system consisting of two CR-39 detectors  $3 \times 4 \text{ cm}^2$  in dimension coupled to a  $^{10}\text{B}$  enriched converter, positioned inside a sphere made with polyethylene, lead, and cadmium. The  $^{10}\text{B}$  is contained in boron carbide ( $\text{B}_4\text{C}$ ) deposited on an aluminum plate. The thickness of the boron carbide is about 10  $\mu\text{m}$ . The instrument is an extended range rem counter and the response function is shown in Fig. 1. The full description of the instrument is in (Caresana et al., 2014) while previous experience in measuring onboard aircraft is described in (Federico et al., 2015).

The plug, hosting the two CR-39 detectors assembled with the boron converter, was removed from the moderating sphere during the shipment, inserted into the sphere immediately before take-off and removed immediately after landing.

A check of the calibration coefficient was performed at CERF in August 2017 and resulted in  $10.6 \text{ cm}^{-2}\cdot\mu\text{Sv}^{-1}$  with an uncertainty equal to 14% ( $k = 1$ ). The sensitivity is about 3 times higher than the one reported in (Caresana et al., 2014). This is because the boron converter used in the above cited work is the Enriched Converter Screen BE10 by Dosirad (France) whose thickness is about 100  $\mu\text{m}$ . Using this converter, only a layer of about 10  $\mu\text{m}$  directly facing the CR-39 detector contributes to the signal, while interactions occurring at longer distance generate reaction products that are self-absorbed in the converter. The effect is a depression of the thermal neutron flux, resulting in a reduced sensitivity.

### 2.3.5. Electronic neutron dosimeter ELDO

The ELDO is an individual dosimeter developed at the Helmholtz Zentrum München (HMGU), sensitive to neutrons from thermal energies up to about 200 MeV (Wielunski et al., 2004). It is a small (160 g,  $115 \times 60 \times 16 \text{ mm}^3$ ) personal dosimeter with a dose measurement range between 1  $\mu\text{Sv}$  and 10 Sv. Its operational lifetime is about 400 h. It consists of four Si PIN-diodes with LiF or polyethylene (PE) converters encapsulated in lead or cadmium. The combination of diodes and converter enables separate measurements of neutrons with one fast-sensor (PE) operating in the 1–200 MeV neutron energy range, two delta-sensors (LiF) functioning between 50 keV and 2 MeV, and one albedo-sensor (LiF) sensitive to low-energy neutrons (<50 keV). Each sensor is sensitive to a certain neutron energy range and has its own calibration factor. The measured dose and dose rate in terms of the personal dose equivalent,  $H_p(10)$  (an operational quantity for individual monitoring for the assessment of effective dose), are also shown on its LCD display. Calibration of the ELDO was done at PTB Braunschweig, Germany, in mono-energetic neutron fields with energies between 138 keV and 14.8 MeV (Bergmeier et al., 2013). Additionally, the ELDO was also tested in the reference field of CERN-CERF providing high-energy fields similar to that of secondary cosmic rays at flight altitudes (Wielunski et al., 2018) and at the Environmental Research Station "UFS Schneefernerhaus" (2650 m above sea level) close to the summit of the Zugspitze Mountain, Germany (Volnhals, 2012). In these experiments, very low impact of

other particles of secondary cosmic rays but neutrons was observed. For example, the protons of secondary cosmic rays at the Zugspitze cause only about 10% of the measured counts. The sensor response to protons and muons has been calculated with GEANT4 simulations (Volnhals, 2012) which support this observation.

## 2.4. Calculations

Ambient dose equivalent rates for different particles can be calculated using various models; the overview of codes assessing radiation exposure of aircraft crew is given in (Bottollier-Depois et al., 2012). All these codes provide calculations for the GCR induced radiation field in aircraft flight altitudes agreeing within 20% with reference measurements (Bottollier-Depois et al., 2012). In this publication, the EPCARD.Net code (Mares et al., 2009) was used for comparison.

### 2.4.1. EPCARD.Net

The European Program package for the Calculation of Aviation Route Doses (EPCARD) is a widely used program for estimating the exposure of aircraft crew. This code was developed at the Helmholtz Zentrum München (Schraube et al., 2002b) and further improved in a new object-oriented code EPCARD.Net (Mares et al., 2009). In 2010, EPCARD.Net ver. 5.4.3 Professional was approved for official use for assessing radiation exposure from secondary cosmic radiation at aviation altitudes by the German Aviation Authority (LBA) and the National Metrology Institute, Physikalisch-Technische Bundesanstalt (PTB).

EPCARD.net is based on the results of extensive FLUKA Monte Carlo (Ferrari et al., 2005; Böhlen et al., 2014) calculations of particle energy spectra of neutrons, protons, photons, electrons and positrons, muons, and pions at various depths in the atmosphere down to sea level for all possible values of solar activity and geomagnetic shielding conditions (Roesler et al., 2002). The primary particle spectra used in the FLUKA calculations as well as the modulation potential describing solar activity were based on the model of Badhwar and O'Neill (Badhwar, 1997; Badhwar et al., 2000).

To determine the dose rates at specific locations in the atmosphere during a flight, the cut-off rigidity, the solar deceleration potential and the barometric altitude are calculated to quantify geomagnetic shielding, solar activity and atmospheric shielding. The EPCARD.Net parameter database includes energy-averaged dose conversion coefficients, calculated by folding each single-particle fluence spectrum with the appropriate dose conversion function (Mares et al., 2004; Mares and Leuthold, 2007), which depends on barometric altitude, cut-off rigidity, and solar activity, since the shape of the particle energy spectra also depends on these parameters. Ambient dose equivalent,  $H^*(10)$ , and effective dose,  $E$ , are calculated separately for each particle, i.e. the dose contributions from neutrons, protons, photons, electrons, muons, and pions are assessed individually.

More general information about EPCARD is available on the web site (EPCARD, 2020), where a simplified on-line version of the EPCARD calculator for public use can also be found.

## 3. Experiment

### 3.1. Flight

The radiation detectors were exposed aboard an Embraer Legacy 600 aircraft operated by ABS Jets. The aircraft, together with 250 kg of equipment and eight scientific staff, flew from Vaclav Havel Airport in Prague (50.1°N, 14.2° E, 380 m AMSL) to the FL390 flight level, on the 29<sup>th</sup> November 2017. The flight took off at the airport at 13:06 UTC and reached stable flight conditions (barometric altitude  $11871 \pm 8$  m (range from 11853 to 11893), latitude  $50.41 \pm 0.14$  °N (range from 50.18 to 50.58), longitude  $15.80 \pm 0.27$ ° E (range from 15.26 to 16.24)) at 13:38 UTC. At this level, the aircraft circled over the northern part of the Czech Republic (the area is a reserved airspace that is commonly

used for operating test flights) for 90 min and landed back at Prague Airport at 15:34 UTC. Navigation data (barometric altitude, latitude, and longitude) were taken from the aircraft record and GPS. The flight route and flight profile are shown in Fig. 2 and Fig. 3, respectively. The space weather conditions were stable during the whole flight and no short-term solar activity affected the results. Space weather situation can be assessed e.g. by neutron monitors (nmdb.eu). During the flight the variation in the count rates of the neutron monitor at Lomnický Stit (the nearest neutron monitor) was below 0.5%, which indicates stable space weather conditions.

### 3.2. Location of detectors inside the aircraft

The detectors were placed at various locations inside the aircraft (Fig. 4). Equipment that needed power and manual control were installed on or behind the seats. Smaller devices like Liulins or Airdos were distributed in various locations inside the aircraft. The rest of the instruments were stored in the baggage compartment.

Two fuel tanks are located in the wings, two fuel tanks are in the bottom part of the body and two fuel tanks are in the rear part of the plane, behind the baggage compartment. Because the flight was quite short (about 2.5 h), only the tanks in the wings were filled with fuel. The total amount of fuel before take-off was 5482 L (4380 kg), 2530 kg were burned during the flight.

## 4. Results and discussion

Not all devices operated during the whole flight, part of the instruments were started when stable flight conditions were reached. To compare the results obtained with the active detectors, we consider only data acquired at a constant flight altitude.

Values of  $H^*(10)$  for various particles calculated with EPCARD are shown in Table 2. It should be noted that the calculations were done in free air, whereas the instruments measured inside the aircraft and therefore small differences can be expected due to shielding effects (Ferrari et al., 2004). As can be seen from Table 2, the most important contribution to  $H^*(10)$  is from neutrons (57% of the total  $H^*(10)$ ), followed by electrons (20%) and protons (15%). The uncertainty on the calculated values is estimated to be less than 20%, based on (Bottollier-Depois et al., 2012) who compared various codes used for assessing radiation exposure of aircraft crew due to GCR with the conclusion that the agreement between the codes was better than 20% from the median. The codes have also been previously validated by measurements with an agreement better than  $\pm 20\%$  (Lindborg et al., 2004).

Table 3 lists the measurement results (for all instruments except Si detectors measuring only  $D_{Si}$ ). The results are grouped in a low-LET component that comprises the contribution of low ionizing radiation (photons, electrons, muons, protons, pions) and in a high-LET component representing mostly contributions of neutrons, stopping protons and higher Z ionizing particles. Even if the neutron contribution can extend below  $10 \text{ keV}\cdot\mu\text{m}^{-1}$  and for low energy photons it can be above  $10 \text{ keV}\cdot\mu\text{m}^{-1}$ , the previous assumption (high-LET assimilated to neutrons) is usually made when comparing results of various instruments and calculations. One should also note that most detectors designed for low-LET measurements exhibit a response to neutrons that is usually unknown, especially for high-energy neutrons. In the table, the results provided are not corrected for this unknown neutron response. Uncertainties are given as combined uncertainties with contributions from calibration and measurement statistics and presented with coverage factor  $k = 1$ . For TEPC, the statistical uncertainty is given in parenthesis. The first group includes instruments routinely used onboard aircraft, measuring both low-LET and high-LET components, the second group includes neutron rem-counters and the third group includes the remaining instruments.

When comparing the results, an agreement of  $\pm 20\%$  at a 95% confidence level is considered satisfactory. The recommendation on

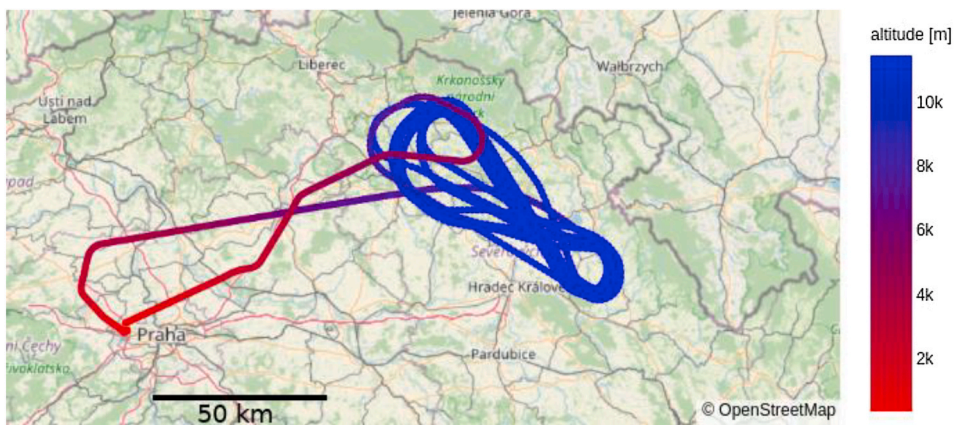


Fig. 2. Flight route.

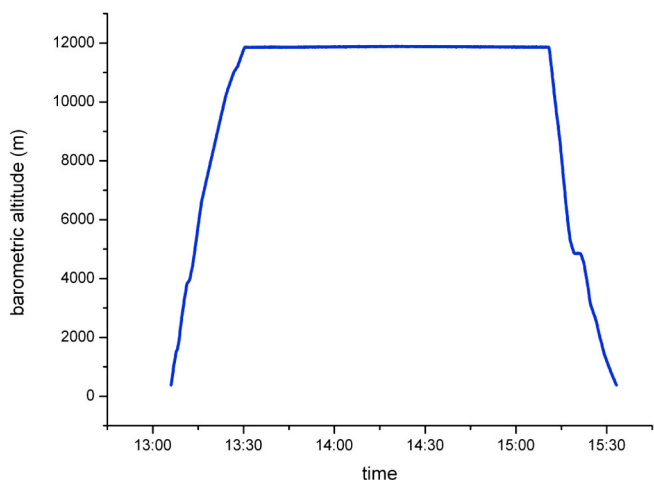


Fig. 3. Flight profile.

acceptable uncertainties in radiation protection is given in (ICRP, 1997) where it is stated: “...overall uncertainty at the 95% confidence level in the estimation of effective dose around the relevant dose limit may well be a factor of 1.5 in either direction for photons and may be substantially greater for neutrons of uncertain energy and for electrons. Greater uncertainties are also inevitable at low levels of effective dose for all qualities of radiation.”

The measurements of the various TEPCs (HAWK, Sievert) agreed well with each other, with Liulin, and with the EPCARD calculations, as it was during a previous flight comparison (CAATER) (Lillhök et al.,

2007). The differences in low-LET and high-LET components between the Sievert instrument and the other TEPCs were likely due to the fact that the Sievert instrument distinguished  $H^*(10)$  contributions from photons and neutrons rather than in terms of a low-LET and high-LET threshold. The differences could have been also due to different locations of the TEPCs (Hawks in the baggage compartment, Sievert in the front of the plane). During the approximately 90 min of the cruise, the TEPC experienced statistically low number of high-LET events, which resulted in higher uncertainties for this component.

The LB6419 and REM-2 measured larger values of total  $H^*(10)$  than the TEPCs. The REM-2 is very sensitive to vibrations, which probably led to the very high value of the uncertainty. In principle, there are recombination methods for separating the dose according to LET, but in this flight, the measurement method was simplified because of the short time and difficult conditions. Provision of the values for the low-LET and high-LET components would be helpful to better interpret the data. Improved calibration is needed to make use of REM-2 for routine aircraft dosimetry.

The LB6419 also measured a higher value of total  $H^*(10)$  than the TEPCs. In addition, Table 3 shows a small measured value of the low-LET

Table 2

Calculated values of  $H^*(10)$  rate during the REFLECT at FL390 for different particles using EPCARD.Net ver. 5.5.0

|  | neutrons      | photons       | protons       | electrons     | muons         | total         |
|--|---------------|---------------|---------------|---------------|---------------|---------------|
| $H^*(10)$<br>[ $\mu\text{Sv}/\text{h}$ ] | $3.8 \pm 0.8$ | $0.3 \pm 0.1$ | $1.0 \pm 0.2$ | $1.3 \pm 0.3$ | $0.2 \pm 0.0$ | $6.6 \pm 1.3$ |

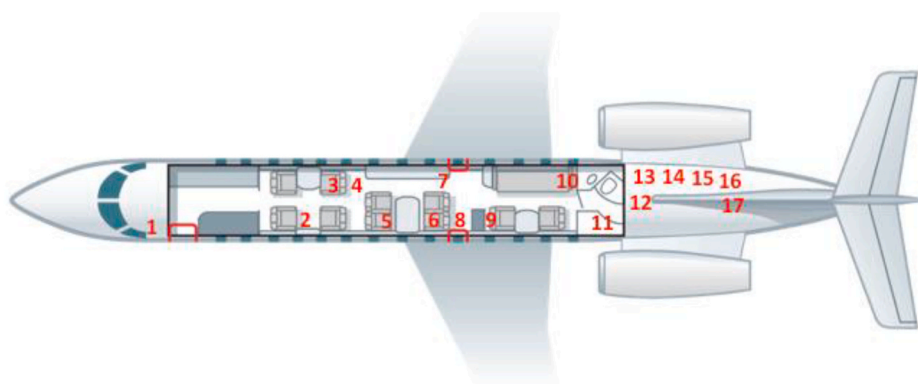


Fig. 4. Placement of detectors inside the aircraft: 1 – Liulin MDU10; 2 – Sievert, 3 – Timepix; 4 – HammerHead; 5 – LB6411; 6 – LB6419; 7 – Liulin MDU7; 8 – NM2B–495 Pb Rem Counter; 9 – Liulin MDU14; 10 – LINUS; 11 – AIRDOS; 12 – REM-2 recombination chamber; 13 – TTM + FH 40 G-10 + FHZ-612B, 14 – ELDO; 15 – TEPC Hawk (IRSN); 16 – passive REM counter + Liulin MDU1; 17 – TEPC Hawk (SL).



**Table 3**

Ambient dose-equivalent rate measured with the various detectors. Uncertainties given as combined uncertainties with  $k = 1$  and with the contribution from measurement statistics in parenthesis.

|                            | Instrument                        | $H^*(10)$<br>[ $\mu\text{Sv/h}$ ] | $H^*(10)_{\text{Low-LET}}$<br>or $H^*(10)_{\gamma+e}$<br>[ $\mu\text{Sv/h}$ ] | $H^*(10)_{\text{High-LET}}$<br>or $H^*(10)_n$<br>[ $\mu\text{Sv/h}$ ] |
|----------------------------|-----------------------------------|-----------------------------------|---|---|
| routinely used instruments | TEPC HAWK (SL)                    | $7.1 \pm 0.5$ (0.3)               | $3.3 \pm 0.1$ (<0.1)  | $3.8 \pm 0.6$ (0.3)   |
|                            | TEPC HAWK (IRSN)                  | $7.9 \pm 0.6$ (0.3)               | $3.5 \pm 0.1$ (<0.1)  | $4.4 \pm 0.5$ (0.3)   |
|                            | Sievert (SSM)                     | $7.4 \pm 0.6$ (0.4)               | $2.9 \pm 0.2$ (0.1)   | $4.5 \pm 0.6$ (0.6)   |
| Neutron rem-counters       | Liulin MDU7 (NPI)                 | $7.1 \pm 1.1$                     | $3.1 \pm 0.5$   | $4.0 \pm 0.7$   |
|                            | NM2B-495 Pb (HMGU)                |                                   |   | $3.7 \pm 0.4$   |
|                            | LINUS (CERN)                      |                                   |   | $3.9 \pm 0.1$   |
|                            | LB6411 (NPI)                      |                                   |   | $2.1 \pm 0.4$   |
|                            | Passive REM counter (Polimi)      |                                   |   | $7.5 \pm 2.5$   |
| Other instruments          | LB6419 (DESY)                     | $9.1 \pm 1.8$                     | $1.7 \pm 0.4$   | $7.4 \pm 1.5$   |
|                            | REM-2 (NCBJ)                      | $10.1 \pm 8.9$                    | –   | –   |
|                            | TTM (NCBJ)                        | $4.8 \pm 0.8$                     | $2.1 \pm 0.4$   | $2.8 \pm 0.5$   |
|                            | ELDO (HMGU)                       |                                   |   | $4.4 \pm 0.9^a$   |
|                            | HammerHead HH (HHtec Association) |                                   | $2.7 \pm 0.2$   |   |
|                            | FH 40 G-10 (NCB)                  |                                   | $3.2 \pm 0.5$   |   |
| FHZ-612B (NCB)             |                                   | $4.7 \pm 0.8$                     |   |   |

<sup>a</sup>  $H_p(10)$ .

radiation contribution and an increased contribution of the high-LET component as compared to the TEPCs. There is a need to check the separation method of the two components and the calibration, since the total ambient dose equivalent was also too high compared to the TEPC.

The  $H^*(10)$  values measured with the TTM monitoring station, especially the neutron component, was lower than the other instruments. Since only polyethylene was used as a moderator (no lead or other high atomic number material was included in the shell), the neutron energy range of this instrument was limited to 20 MeV.

Except for the LB6411 and TTM, the instruments measuring only the neutron component provided results comparable to the TEPC results and with the EPCARD calculations.

According to the EPCARD model, neutrons contributed for more than 50% to the total  $H^*(10)$ ; neutrons can reach energies up to several hundreds of MeV (Pazianotto et al., 2017). Conventional neutron REM counters have a detection range usually limited to about 15–20 MeV, their response dropping sharply at higher energies. To extend the range to higher energies (up to several hundreds of MeV), a shell of high-Z material (like tungsten or lead) is usually added to the PE moderator.

As expected, due to their response functions (Fig. 1), the LB6411 and TTM measured lower values. This was in agreement also with measurements by Yasuda and Yajima (2018), who investigated neutron doses during long-haul flights with two neutron monitors and compared their results with JISCARD EX calculations. They found that the relative contribution to  $H^*(10)$  of neutrons with energies above 15 MeV could exceed 50%.

The passive REM counter only provided an integral value over the whole flight (the detector was installed inside the moderator just before take-off and removed after landing). The total measured  $H^*(10)$  was  $15 \pm 5 \mu\text{Sv}$ ; the dose rate at flight level FL390 can be assessed assuming a taxi time of about 2 h and neglecting the small contribution arising from the 0.5 h spent to reach the flight altitude and get back to ground.

A possible explanation of the large measured  $H^*(10)$  value is that the passive REM counter – because of a misunderstanding with the shipping company – reached Prague by airmail. Of course, the plug with the

detector was not in the measuring position, thus insensitive to fast neutrons. However, a small contribution from thermal neutrons cannot be excluded.

Amongst the instruments measuring only the low-LET component, only the HammerHead HH and the FH 40 G-10 obtained reasonable results. The results from the other instruments disagreed with both the EPCARD calculation and the TEPC measurements. It is difficult to compare the results because some photon detectors are not only sensitive to photons and electrons, but also to protons, muons, pions and to neutrons in some extent. For these instruments, their response to components of the field other than that intended to be measured is not always known.

Table 4 summarises the results of the silicon detectors (in terms of absorbed dose). For these instruments, the dose in silicon was converted to dose in water using a dose conversion factor of 1.23 (Ploc, 2009). In a previous intercomparison flight with Liulin MDUs (Meier et al., 2016) it was found that there could be differences in the mass of the sensitive volume of the detectors (Si sensor size) considered in the calculation of absorbed dose. In this experiment, we calculated the absorbed dose in silicon using the same Si sensor mass (0.16597 g (Meier et al., 2016)) for all Liulin units and for Airdos.

Although both Liulin and Airdos have similar sensitive volumes (mass, area, thickness), they have different properties such as energy range of deposited energy and width of the channel. Airdos has channel width of 49.4 keV whereas Liulin's is 81.4 keV. The energy range of Airdos (up to 12 MeV) is smaller than Liulin's (up to 24 MeV), in order to provide more detailed information on the lower part of the energy spectrum. The significant part of the deposited energy when measuring onboard aircraft comes from events depositing energy in the first several channels (for Liulins, 65–83% of the absorbed dose was due to events with deposited energy below 1 MeV, only 2–6% was due to events with deposited energy above 10 MeV).

To compare Airdos with Liulin, we considered only events within the energy range of Airdos for the calculation of absorbed dose for Liulin. For MDU 7,  $D_{\text{Si}}$  was  $2.6 \mu\text{Gy}\cdot\text{h}^{-1}$ , for MDU 10  $D_{\text{Si}}$  was  $1.9 \mu\text{Gy}\cdot\text{h}^{-1}$ , and for MDU 14  $D_{\text{Si}}$  was  $2.6 \mu\text{Gy}\cdot\text{h}^{-1}$ , to be compared with  $1.8 \mu\text{Gy}\cdot\text{h}^{-1}$  measured by Airdos.

Some differences in the results could be due to the different shielding configurations (for example, the aircraft fuel acts as a good neutron moderator) around the locations in which the devices were installed (Fig. 4). The DLR Liulin was in the baggage compartment, whereas the NPI Liulin and the Airdos were in the central part of the aircraft or in the crew cabin. For Embraer Legacy 600, the baggage compartment is located in the rear part of the aircraft, between the engines (Fig. 4). Therefore, the baggage compartment, loaded with several larger instruments and suitcases, is supposed to be more shielded than other areas of the aircraft. As was shown in Ferrari et al. (2004), the shielding provided by the aircraft structure (wings, engines, passengers, fuel) can cause a notable reduction in  $E$  or  $H^*(10)$  for most components of cosmic radiation. Differences in ambient dose equivalent for various places inside the aircraft can be up to about 20% (Ferrari et al., 2004; Battistoni

**Table 4**

Results (absorbed dose rate in silicon and in water) of the measurements with the Silicon detectors.

| Instrument   | MDU 7<br>Liulin<br>(NPI) | MDU<br>10<br>Liulin<br>(QST) | MDU14<br>Liulin<br>(QST) | MDU1<br>Liulin<br>(DLR) | Airdos<br>T4<br>(NPI) | Minipix<br>(NPI) |
|--|--------------------------|------------------------------|--------------------------|-------------------------|-----------------------|------------------|
| $D_{\text{Si}}$ ( $\mu\text{Gy/h}$ )                       | $2.8 \pm 0.2$            | $2.1 \pm 0.3$                | $2.7 \pm 0.5$            | $2.0 \pm 0.3$           | $1.8 \pm 0.2$         | $1.9 \pm 0.3$    |
| $D_{\text{H}_2\text{O}}$ ( $\mu\text{Gy/h}$ ) <sup>a</sup> | $3.4 \pm 0.3$            | $2.6 \pm 0.4$                | $3.4 \pm 0.6$            | $2.5 \pm 0.3$           | $2.2 \pm 0.2$         | $2.3 \pm 0.3$    |

<sup>a</sup> The dose  $D_{\text{H}_2\text{O}}$  was calculated from  $D_{\text{Si}}$  using conversion factor 1.23 (the factor was applied to unrounded value of  $D_{\text{Si}}$  and then  $D_{\text{H}_2\text{O}}$  were rounded to significant digits).

et al., 2005; Kubančák et al., 2014). Nevertheless, the differences between individual Liulin-type detectors seem to be too large to be explained only by different locations in the aircraft. There appears to be some systematic differences. The reason of these differences should be further investigated in comparison on ground. Even for the detectors using the same Si diode, several factors can influence the results, e.g. energy calibration, choice of the noise threshold, channel width (Kákona et al., 2019).

Although the Minipix has larger energy range (from 5 keV), it showed a lower absorbed dose than the MDUs. This is difficult to explain since the Minipix was calibrated against the TEPC and showed a very good agreement to the TEPC Hawk low-LET part (Ploc, 2009). However, it should be mentioned that the setting of Timepix, especially bias, could have been different for different experiments, which might have caused some discrepancies. In this flight, the bias was set to 30 V. It was important to use the same conditions (parameters) for all instruments.

Taking the MDU7 (MDU 7 has been calibrated at CERF) energy deposition spectra and performing the calibration according to (Ploc, 2009), the total  $H^*(10)$  rate arrived at  $7.1 \mu\text{Sv}\cdot\text{h}^{-1}$ , which agreed well with the TEPC results.

## 5. Conclusions

For the instruments with the potential to be used onboard aircraft, appropriate calibration and determination of calibration/correction factor are crucial. A good measurement of the atmospheric ambient dose equivalent requires that the instrument response for all particles and energies is properly taken into account. As there is no traceable reference field for the total radiation field in the atmosphere, comparison of instruments onboard aircraft is necessary.

Various radiation detector systems were compared onboard aircraft under stable flight conditions during the REFLECT measurement campaign – the largest comparison of this type ever performed. As expected, the dosimeters routinely used for aircraft dosimetry and for code verifications (TEPC, Liulin) worked adequately, the results agreed with each other as well as with the EPCARD computer model calculations.

Since high-energy neutrons contribute significantly to  $H^*(10)$ , conventional neutron rem counters (with energy range limited to about 20 MeV) underestimated neutron  $H^*(10)$  with standard calibration procedures using neutron sources such as Am–Be or  $^{252}\text{Cf}$ . Extended-range neutron rem counters (NM2B–495 Pb, LINUS) provided results comparable to  $H^*(10)_n$  determined with routinely used instruments and the EPCARD calculation.

The reading of some instruments (LB6419, FHZ-612B) was higher than expected from the assumption that the detector is only sensitive to a specific component of the radiation field. However, it should be noted that these instruments are not primarily intended for use onboard aircraft in a very complex mixed radiation field. Their response to the various components of the cosmic radiation field and the energy dependence still need to be fully characterised.

The REFLECT campaign enabled measurement in uniform, well-defined conditions onboard an aircraft and comparison of new instruments with those routinely used. Although the response of some instruments that are not routinely used for onboard aircraft dosimetry was different compared to the response of those routinely used, more experiments are necessary either to declare them as not suitable or to develop procedures enabling them for such use. This campaign consisted only of one flight with one set of parameters (vertical cut-off rigidity, altitude, phase of solar cycle) and it was relatively short. For further testing of instruments showing some potential to be used for routine dosimetry onboard aircraft, additional flights at different geomagnetic cut-offs and altitudes as well as comparison at appropriate reference fields (CERF) are needed. The REFLECT provided valuable experience enabling to discuss some issues connected with the use of the dosimeters in such complex radiation field and it also provided feedback for more rigorous validation of calculated aviation doses.

## Declaration of competing interest

The authors declare that they have no known competing financial interests or personal relationships that could have appeared to influence the work reported in this paper.

## Acknowledgements

The research flight has been part of the research activities of the CRREAT (Research Center of Cosmic Rays and Radiation Events in the Atmosphere) project funded by the European Structural and Investment Funds under the Operational Program Research, Development and Education (CZ.02.1.01/0.0/0.0/15\_003/0000481).

This work was carried out within the European Radiation Dosimetry Group (EURADOS, WG11 High energy radiation fields).

We would like to thank ABSJets pilots and technicians for their assistance during the flight and its preparation.

## References

- Andersson, I.O., Braun, J.A., 1963. Neutron rem-counter with uniform sensitivity from 0.025 eV to 10 MeV. In: *Proceedings of the IAEA Symposium on Neutron Dosimetry*, vol. II. IAEA, Vienna, pp. 87–95.
- Badhwar, G.D., 1997. The radiation environment in low-Earth orbit. *Radiat. Res.* 148, 3–10. <https://doi.org/10.2307/3579710>.
- Badhwar, G.D., O'Neill, P.M., Troung, A.G., 2000. *Galactic Cosmic Radiation Environmental Models*, Private Communication.
- Battistoni, G., Ferrari, A., Pelliccioni, M., Villari, R., 2005. Evaluation of the doses to aircrew members taking into consideration the aircraft structures. *Adv. Space Res.* 36, 1645–1652. <https://doi.org/10.1016/j.asr.2005.04.037>.
- Beck, P., 2009. Overview of research on aircraft crew dosimetry during the last solar cycle. *Radiat. Protect. Dosim.* 136, 244–250. <https://doi.org/10.1093/rpd/ncp158>.
- Beck, P., Latocha, M., Rollet, S., Stehno, G., 2005. TEPC reference measurements at aircraft altitudes during a solar storm. *Adv. Space Res.* 36, 1627–1633. <https://doi.org/10.1016/j.asr.2005.05.035>.
- Bengtsson, L.G., 1970. Assessment of dose equivalent from fluctuation of energy depositions. In: *Proc. 2nd Symp. On Microdosimetry EUR-4552 (Brussels: CEC)*, pp. 375–400.
- Bergmeier, F., Volnhals, M., Wielunski, M., Rühm, W., 2013. Simulation and calibration of an active neutron dosimeter. *Radiat. Protect. Dosim.* 161, 126–129. <https://doi.org/10.1093/rpd/nct316>.
- ERTHOLD n.d., LB 6411 Neutron Probe, Berthold Technologies USA, accessed 14 April 2020, <<http://www.berthold-us.com/50-rad-pro-products/probes-sensors/156-lb-6411.html>>.
- Birattari, C., Ferrari, A., Nuccetelli, C., Pelliccioni, M., Silari, M., 1990. An extended range neutron rem counter. *Nucl. Instrum. Methods Phys. Res.* 297, 250–257. [https://doi.org/10.1016/0168-9002\(90\)91373-J](https://doi.org/10.1016/0168-9002(90)91373-J).
- Birattari, C., Esposito, A., Ferrari, A., Pelliccioni, M., Silari, M., 1992. A neutron survey-meter with sensitivity extended up to 400 MeV. *Radiat. Protect. Dosim.* 44, 193–197. <https://doi.org/10.1093/rpd/44.1-4.193>.
- Birattari, C., Esposito, A., Ferrari, A., Pelliccioni, M., Silari, M., 1993. Calibration of the neutron rem counter LINUS in the energy range from thermal to 19 MeV. *Nucl. Instrum. Methods Phys. Res.* 324, 232–238. [https://doi.org/10.1016/0168-9002\(93\)90982-N](https://doi.org/10.1016/0168-9002(93)90982-N).
- Birattari, C., Esposito, A., Ferrari, A., Pelliccioni, M., Rancati, T., Silari, M., 1998. The extended range Neutron rem counter 'LINUS': overview and latest developments. *Radiat. Protect. Dosim.* 76, 135–148. <https://doi.org/10.1093/oxfordjournals.rpd.a032258>.
- Böhlen, T.T., Cerutti, F., Chin, M.P.W., Fassò, A., Ferrari, A., Ortega, P.G., Mairani, A., Sala, P.R., Smirnov, G., Vlachoudis, V., 2014. The FLUKA code: developments and challenges for high energy and medical applications. *Nucl. Data Sheets* 120, 211–214. <https://doi.org/10.1016/j.nds.2014.07.049>.
- Bottollier-Depois, J.-F., Tromprier, F., Clairand, I., Spurny, F., Bartlett, D., Beck, P., Lewis, B., Lindborg, L., O'Sullivan, D., Roos, H., Tommasino, L., 2004. Exposure of aircraft crew to cosmic radiation: on-board intercomparison of various dosimeters. *Radiat. Protect. Dosim.* 110, 411–415. <https://doi.org/10.1093/rpd/nch217>.
- Bottollier-Depois, J.F., Beck, P., Latocha, M., Mares, V., Matthia, D., Rühm, W., Wissmann, F., 2012. Comparison of Codes Assessing Radiation Exposure of Aircraft Crew Due to Galactic Cosmic Radiation. *EURADOS Report 2012-03*. Braunschweig, May 2012. ISBN 978-3-943701-02-9.
- Bottollier-Depois, J.F., Allain, E., Baumont, G., Berthelot, N., Darley, G., Ecrabet, F., Jolivet, T., Lebeau-Livé, A., Lejeune, V., Quéinnec, F., Simon, C., Tromprier, F., 2019. The OpenRadiation project: monitoring radioactivity in the environment by and for the citizens. *Radioprotection* 54, 241–246. <https://doi.org/10.1051/radiopro/2019046>.
- Burgkhardt, B., Fieg, G., Klett, A., Plewnia, A., Siebert, B.R.L., 1997. The neutron fluence and  $H^*(10)$  response of the new LB 6411 rem counter. *Radiat. Protect. Dosim.* 70, 361–364. <https://doi.org/10.1093/oxfordjournals.rpd.a031977>.
- Campbell, M., On behalf of all members of the Medipix2 collaboration, 2011. 10 years of the Medipix2 collaboration. *Nucl. Instrum. Methods Phys. Res. Sect. A Accel.*

- Spectrom. Detect. Assoc. Equip. 633, S1–S10. <https://doi.org/10.1016/j.nima.2010.06.106>.
- Caresana, M., Denker, A., Esposito, A., Ferrarini, M., Golnik, N., Hohmann, E., Leuschner, A., Luszik-Bhadra, M., Manessi, G., Mayer, S., Ott, K., Röhrich, J., Silari, M., Tromprier, F., Volnhals, M., Wielunski, M., 2014. Intercomparison of radiation protection instrumentation in a pulsed neutron field. *Nucl. Instrum. Methods Phys. Res. Sect. A Accel. Spectrom. Detect. Assoc. Equip.* 737, 203–213. <https://doi.org/10.1016/j.nima.2013.11.073>.
- Conroy, T., 2004. FWT Far West Technology Inc., Environmental Radiation Monitor with 500 Tissue Equivalent Proportional Counter (TEPC), HAWK Version 2. *Operations and Repair Manual*. Far West Technology, Inc., Goleta, USA.
- CRREAT. n.d. The CRREAT project, nuclear Physics institute CAS. accessed 14 April, 2020. <http://www.ujf.cas.cz/en/research-development/large-research-infrastructure-and-centres/crreat/objectives/>.
- Dachev, T.P., 2009. Characterization of the near Earth radiation environment by Liulin type spectrometers. *Adv. Space Res.* 44, 1441–1449. <https://doi.org/10.1016/j.asr.2009.08.007>.
- Dinar, N., Pozzi, F., Silari, M., 2017. Characterization of the LINUS detector. CERN-RP-2017-060-REPORTS-TN. EDMS 1822865.
- E, PCARD, 2020. *EPCARD Online*, Helmholtz Zentrum Muenchen accessed 14 April 2020. <https://www.helmholtz-muenchen.de/epcard>.
- EURADOS, 1996. In: McAulay, I.R., Bartlett, D.T., Dietre, G., Menzel, H.G., Schnuer, K., Schrewe, H.J. (Eds.), *Exposure of Air Crew to Cosmic Radiation*. Luxembourg, ISBN 92-827-7994-7.
- E, URADOS, 2020. the European Radiation Dosimetry Group. EURADOS accessed 14 April 2020. <https://eurados.skcken.be/en>.
- EURATOM, 1996. Council Directive 96/29/EURATOM of 13 May 1996 laying down the basic safety standards for protection of the health of workers and the general public against the dangers arising from ionising radiation. *Off. J. Eur. Communities* 39, L159.
- EURATOM, 2013. Council Directive 2013/59/EURATOM of 5 December 2013 laying down basic safety standards for protection against the dangers arising from exposure to ionising radiation, and repealing Directives 89/618/Euratom, 90/641/Euratom, 96/29/Euratom, 97/43/Euratom and 2003/122/Euratom. *Orkesterjournalen L* 13, 17.1.2014.
- Farah, J., De Saint-Hubert, M., Mojszesz, N., Chiriotti, S., Gryzinski, M., Ploc, O., Tromprier, F., Turek, K., Vanhavere, F., Olko, P., 2017. Performance tests and comparison of microdosimetric measurements with four tissue-equivalent proportional counters in scanning proton therapy. *Radiat. Meas.* 96, 42–52. <https://doi.org/10.1016/j.radmeas.2016.12.005>.
- Federico, C.A., Gonzalez, O.L., Caldas, L.V.E., Pazianotto, M.T., Dyer, C., Caresana, M., Hands, A., 2015. Radiation measurements onboard aircraft in the South Atlantic region. *Radiat. Meas.* 82, 14–20. <https://doi.org/10.1016/j.radmeas.2015.07.008>.
- Ferrari, A., Pelliccioni, M., Villari, R., 2004. Evaluation of the influence of aircraft shielding on the aircrew exposure through an aircraft mathematical model. *Radiat. Protect. Dosim.* 108, 91–105. <https://doi.org/10.1093/rpd/nch008>.
- Ferrari, A., Sala, P.R., Fasso, A., Ranft, J., 2005. FLUKA: A Multi Particle Transport Code. CERN-2005-010, SLAC-R-773, INFN-TC-05-11. <https://doi.org/10.2172/877507>.
- GitHub, 2020. *ODZ-UJF-AV-CR/AIRDOS01: Airborne Cosmic Radiation Dosimeter*. GitHub, Inc. accessed 14 April 2020. <https://github.com/ODZ-UJF-AV-CR/AIRDOS01>.
- Golnik, N., 2018. Recombination chambers - do the old ideas remain useful? *Radiat. Protect. Dosim.* 180, 3–9. <https://doi.org/10.1093/rpd/ncx279>.
- Golnik, N., Brede, H.J., Guldbakke, S., 1997. H\*(10) Response of the REM-2 Recombination Chamber in Monoenergetic Neutron Fields. *Radiation Protection Dosimetry* 74 (3), 139–144. <https://doi.org/10.1093/oxfordjournals.rpd.a032189>.
- Golnik, N., Mayer, S., Zielczyński, M., 2004. Recombination index of radiation quality of low-LET radiation. *Nucl. Instrum. Methods Phys. Res. Sect. B Beam Interact. Mater. Atoms* 213, 650–653. [https://doi.org/10.1016/S0168-583X\(03\)01679-3](https://doi.org/10.1016/S0168-583X(03)01679-3).
- Granja, C., Pospisil, S., 2014. Quantum dosimetry and online visualization of X-ray and charged particle radiation in commercial aircraft at operational flight altitudes with the pixel detector Timepix. *Adv. Space Res.* 54, 241–251. <https://doi.org/10.1016/j.asr.2014.04.006>.
- Granja, C., Kudela, K., Jakubek, J., Krist, P., Chvatil, D., Stursa, J., Polansky, S., 2018. Directional detection of charged particles and cosmic rays with the miniaturized radiation camera MiniPIX timepix. *Nucl. Instrum. Methods Phys. Res. Sect. A Accel. Spectrom. Detect. Assoc. Equip.* 911, 142–152. <https://doi.org/10.1016/j.nima.2018.09.140>.
- IAEA, 2003. Occupational radiation protection: protecting workers against exposure to ionizing radiation. *Proceedings of an International Conference Held in Geneva, Switzerland*, pp. 26–30. August 2002. STI/PUB/1145.
- ICRP, 1991. 1990 recommendations of the international commission on radiological protection. *Ann. ICRP* 21 (1–3). ICRP Publication 60.
- ICRP, 1997. General principles for the radiation protection of workers. ICRP publication 75. *Ann. ICRP* 27 (1).
- ICRP, 2007. The 2007 Recommendations of the International Commission on Radiological Protection, vol. 103. ICRP publication.
- ICRP, 2016. Radiological protection from cosmic radiation in aviation. ICRP publication 132. *Ann. ICRP* 45 (1), 1–48.
- ICRU, 1993. Quantities and Units in Radiation Protection Dosimetry. ICRU Report, vol. 51. ICRU Publications, Bethesda.
- ISO, 1999. X and Gamma Reference Radiation for Calibrating Dosimeters and Doserate Meters and for Determining Their Response as a Function of Photon Energy — Part 3: Calibration of Area and Personal Dosimeters and the Measurement of Their Response as a Function of Energy and Angle of Incidence. ISO 4037-3:1999.
- ISO, 2001. Reference Neutron Radiations — Part 1: Characteristics and Methods of Production. ISO 8529-1:2001.
- ISO, 2012. Dosimetry for Exposures to Cosmic Radiation in Civilian Aircraft — Part 1: Conceptual Basis for Measurements. ISO 20785-1:2012.
- Jakubek, J., 2011. Precise energy calibration of pixel detector working in time-over-threshold mode. *Nucl. Instrum. Methods Phys. Res.* 633, S262–S266. <https://doi.org/10.1016/j.nima.2010.06.183>.
- Kákona, M., Štěpán, V., Ambrožová, I., Arsov, T., Chroust, J., Kákona, J., Kalapov, I., Krist, P., Lužová, M., Nikolova, N., Brabcová, D., Ploc, O., Sommer, M., Šlegl, J., Angelov, C., 2019. Comparative measurements of mixed radiation fields using Liulin and AIRDOS dosimeters. In: AIP Conference Proceedings vol. 2075, 130003. <https://doi.org/10.1063/1.5091288>.
- Kellerer, A.M., 1968. *Mikrodosimetrie GSF-Bericht B-1* (Forschungszentrum für Umwelt und Gesundheit).
- Kellerer, A.M., Rossi, H.H., 1984. On the determination of microdosimetric parameters in time-varying radiation fields: the variance-covariance method. *Radiat. Res.* 97, 237–245. <https://doi.org/10.2307/3576275>.
- Kubancák, J., Ambrožová, I., Ploc, O., Brabcová, K.P., Štěpán, V., Uchihori, Y., 2014. Measurement of dose equivalent distribution on board commercial jet aircraft. *Radiat. Protect. Dosim.* 162, 215–219. <https://doi.org/10.1093/rpd/nct331>.
- Kubancák, J., Ambrožová, I., Pachnerová Brabcová, K., Jakubek, J., Kyselová, D., Ploc, O., Bemš, J., Štěpán, V., Uchihori, Y., 2015. Comparison of cosmic rays radiation detectors on-board commercial jet aircraft. *Radiat. Protect. Dosim.* 164, 484–488. <https://doi.org/10.1093/rpd/ncv331>.
- Kyllönen, J.-E., Lindborg, L., Samuelson, G., 2001a. The response of the Sievert instrument in neutron beams up to 180 MeV. *Radiat. Protect. Dosim.* 94 (3), 227–232. <https://doi.org/10.1093/oxfordjournals.rpd.a006494>.
- Kyllönen, J.-E., Lindborg, L., Samuelson, G., 2001b. Cosmic Radiation Measurements on-board aircraft with the variance method. *Radiat. Protect. Dosim.* 93 (3), 197–205. <https://doi.org/10.1093/oxfordjournals.rpd.a006430>.
- Latocha, M., Autischer, M., Beck, P., Bottolier-Depois, J.F., Rollet, S., Tromprier, F., 2007. The results of cosmic radiation in-flight TEPC measurements during the CAATER flight campaign and comparison with simulation. *Radiat. Protect. Dosim.* 125 (1–4), 412–415. <https://doi.org/10.1093/rpd/ncl123>.
- Leake, J.W., 1966. A spherical dose equivalent neutron detector. *Nucl. Instrum. Methods* 45, 151–156. [https://doi.org/10.1016/0029-554X\(66\)90420-4](https://doi.org/10.1016/0029-554X(66)90420-4).
- Leake, J.W., 2004. Improvements to the Leake neutron detector I. *Nucl. Instrum. Methods Phys. Res. Sect. A Accel. Spectrom. Detect. Assoc. Equip.* 519 (3), 636–646. <https://doi.org/10.1016/j.nima.2003.11.040>.
- Leuschner, A., Asano, Y., Klett, A., 2017. Calibration of the radiation monitors from DESY and Spring-8 at the quasi-mono-energetic neutron beams using 100 and 300 MeV <sup>7</sup>Li (p,n) reaction at RCNP in Osaka Japan in November 2014. In: EPJ Web of Conferences, vol. 153, 08017. <https://doi.org/10.1051/epjconf/201715308017>.
- Lillhök, J.E., 2007. *The Microdosimetric Variance-Covariance Method Used for Beam Quality Characterization in Radiation Protection and Radiation Therapy*. PhD thesis. ISBN 91-7155-391-6.
- Lillhök, J., Beck, P., Bottolier-Depois, J.F., Latocha, M., Lindborg, L., Roos, H., Roth, J., Schraube, H., Spurny, F., Stehno, G., Tromprier, F., Wissmann, F., 2007. A comparison of ambient dose equivalent meters and dose calculations at constant flight conditions. *Radiat. Meas.* 42, 323–333. <https://doi.org/10.1016/j.radmeas.2006.12.011>.
- Lillhök, J., Persson, L., Andersen, C.E., Dasu, A., Ardenfors, O., 2017. Radiation protection measurements with the variance-covariance method in the stray radiation fields from photon and proton therapy facilities. *Radiat. Protect. Dosim.* 180 (1–4), 338–341. <https://doi.org/10.1093/rpd/ncx194>.
- Lindborg, L., Bengtsson, L.G., 1971. Development of a microdosimetry system for use with high energy electron beams. In: *Proceedings of the Third Symposium on Microdosimetry*. EUR 4810 d-Fe.
- Lindborg, L., Kyllönen, J.E., Beck, P., Bottolier, J.F., Gerdung, S., 1999. The use of TEPC for reference dosimetry. *Radiat. Protect. Dosim.* 86, 285–288. <https://doi.org/10.1093/oxfordjournals.rpd.a032959>.
- Lindborg, L., Bartlett, D.T., Beck, P., McAulay, I.R., Schnuer, K., Schraube, H., Spurny, F., 2004. Cosmic Radiation Exposure of Aircraft Crew: Compilation of Measured and Calculated Data. Final Report of the EURADOS WG 5. European Commission, Directorate-General for Energy and Transport, Radiation Protection Issue No. 140, Luxembourg. ISBN 92-894-8448-9.
- Lindborg, L., Beck, P., Bottolier-Depois, J.F., Latocha, M., Lillhök, J., Rollet, S., Roos, H., Roth, J., Schraube, H., Spurny, F., Stehno, G., Tromprier, F., Wissmann, F., 2007. Determinations of H\*(10) and its dose components onboard aircraft. *Radiat. Protect. Dosim.* 126 (1–4), 577–580. <https://doi.org/10.1093/rpd/ncm117>.
- Llopert, X., Campbell, M., Dinapoli, R., San Segundo, D., Pernigotti, E., 2002. Medipix2: a 64-k pixel readout chip with 55-um square elements working in single photon counting mode. *IEEE Trans. Nucl. Sci.* 49 (5), 2279–2283. <https://doi.org/10.1109/TNS.2002.803788>.
- Llopert, X., Ballabriga, R., Campbell, M., Tlustos, L., Wong, W., 2007. Timepix, a 65k programmable pixel readout chip for arrival time, energy and/or photon counting measurements. *Nucl. Instrum. Methods Phys. Res. Sect. A Accel. Spectrom. Detect. Assoc. Equip.* 581, 485–494. <https://doi.org/10.1016/j.nima.2007.08.079>.
- Maciak, M., 2018. Calculation of LET distributions in the active volume of a recombination chamber. *Radiat. Protect. Dosim.* 180 (1–4), 407–412. <https://doi.org/10.1093/rpd/ncy073>.
- Mares, V., Leuthold, G., 2007. Altitude-dependent dose conversion coefficients in EPCARD. *Radiat. Protect. Dosim.* 126 (1–4), 581–584. <https://doi.org/10.1093/rpd/ncm118>.
- Mares, V., Sannikov, A.V., Schraube, H., 2002. Response function of the Anderson-Braun and extended range rem counters for neutron energies from thermal to 10 GeV. *Nucl. Instrum. Methods Phys. Res., Sect. A* 476, 341–346. [https://doi.org/10.1016/S0168-9002\(01\)01459-0](https://doi.org/10.1016/S0168-9002(01)01459-0).

- Mares, V., Roesler, S., Schraube, H., 2004. Averaged particle dose conversion coefficient in air crew dosimetry. *Radiat. Protect. Dosim.* 110 (1–4), 371–376. <https://doi.org/10.1093/rpd/nch137>.
- Mares, V., Maczka, T., Leuthold, G., Rühm, W., 2009. Air crew dosimetry with a new version of EPCARD. *Radiat. Protect. Dosim.* 136 (4), 262–266. <https://doi.org/10.1093/rpd/ncp129>.
- Mares, V., Trinkl, S., Iwamoto, Y., Masuda, A., Matsumoto, T., Hagiwara, M., Satoh, D., Yashima, H., Shima, T., Nakamura, T., 2017. Neutron spectrometry and dosimetry in 100 and 300 MeV quasimono-energetic neutron field at RCNP. In: Osaka University, Japan. EPJ Web of Conferences vol. 153, 08020. <https://doi.org/10.1051/epjconf/201715308020>.
- Meier, M.M., Hubiak, M., Matthia, D., Wirtz, M., Reitz, G., 2009. Dosimetry at aviation altitudes (2006–2008). *Radiat. Protect. Dosim.* 136 (4), 251–255. <https://doi.org/10.1093/rpd/ncp142>.
- Meier, M.M., Tromprier, F., Ambrozova, I., Kubancak, J., Matthia, D., Ploc, O., Santen, N., Wirtz, M., 2016. CONCORD: comparison of cosmic radiation detectors in the radiation field at aviation altitudes. *J. Space Weather Space Clim.* 6, A24. <https://doi.org/10.1051/swsc/2016017>.
- Meier, M.M., Copeland, K., Matthia, D., Mertens, C.J., Schennetten, K., 2018. First steps toward the verification of models for the assessment of the radiation exposure at aviation altitudes during quiet space weather conditions. *Space Weather* 16, 1269–1276. <https://doi.org/10.1029/2018SW001984>.
- Murawski, L., Maciak, M., Gryziński, M.A., Domański, S., 2018. Investigation on radiation shielding properties of special concrete in neutron fields. *Radiat. Protect. Dosim.* 180 (1–4), 413–416. <https://doi.org/10.1093/rpd/ncy012>.
- Operational Procedure, M.-1, 15 March 2017. Measurement of Dose Equivalent in Mixed Radiation Field with REM-2 Recombination Chamber, Radiation Protection Measurements Laboratory. National Centre for Nuclear Research.
- Pazianotto, M.T., Cortes-Giraldo, M.A., Federico, C.A., Hubert, G., Gonzalez, O.L., Quesada, J.M., Carlson, B.V., 2017. Extensive air shower Monte Carlo modeling at the ground and aircraft flight altitude in the South Atlantic Magnetic Anomaly and comparison with neutron measurements. *Astropart. Phys.* 88, 17–29. <https://doi.org/10.1016/j.astropartphys.2016.12.004>.
- Ploc, O., 2009. Measurement of Exposure to Cosmic Radiation at Near-Earth Vicinity with Energy Deposition Spectrometer Liulin Onboard Aircrafts and Spacecrafts. PhD thesis. Czech Technical University, Prague.
- Ploc, O., Brabcova, K., Spurny, F., Malusek, A., Dachev, T., 2011. Use of energy deposition spectrometer Liulin for individual monitoring of aircrew. *Radiat. Protect. Dosim.* 144, 611–614. <https://doi.org/10.1093/rpd/ncq505>.
- Ploc, O., Ambrozova, I., Kubancak, J., Kovar, I., Dachev, T.P., 2013. Publicly available database of measurements with the silicon spectrometer Liulin onboard aircraft. *Radiat. Meas.* 58, 107–112. <https://doi.org/10.1016/j.radmeas.2013.09.002>.
- Pozzi, F., Silari, M., 2019. The CERN-EU High-Energy Reference Field (CERF) Facility: New FLUKA Reference Values of Spectral Fluences, Present and Newly Proposed Operational Quantities. submitted for publication in NIM A.
- Pozzi, F., Carbonez, P., Macián-Juan, R., 2015. CERN Radiation Protection (RP) Calibration Facilities. CERN-THESIS-2015-394.
- Pozzi, F., Garcia Alia, R., Brugger, M., Carbonez, P., Danzeca, S., Gkotse, B., Jaekel, M.R., Ravotti, F., Silari, M., Tali, M., 2017. CERN irradiation facilities. *Radiat. Protect. Dosim.* 80 (1–4), 120–124. <https://doi.org/10.1093/rpd/ncx187>.
- Pszona, S., Bantsar, A., Tulik, P., Wincel, K., Zaręba, B., 2014. Low-level gamma and neutron monitoring based on use of proportional counter filled with  $^3\text{He}$  in polythene moderator: study of the responses to gamma and neutrons. *Radiat. Protect. Dosim.* 161 (1–4), 237–240. <https://doi.org/10.1093/rpd/nct274>.
- Roesler, S., Heinrich, W., Schraube, H., 1998. Calculation of radiation fields in the atmosphere and comparison to experimental data. *Radiat. Res.* 149 (1), 87–97. <https://doi.org/10.2307/3579685>.
- Roesler, S., Heinrich, W., Schraube, H., 2002. Monte Carlo calculation of the radiation field at aircraft altitudes. *Radiat. Protect. Dosim.* 98 (4), 367–388. <https://doi.org/10.1093/oxfordjournals.rpd.a006728>.
- Schraube, H., Heinrich, W., Leuthold, G., Mares, V., Roesler, S., 2000. Aviation route dose calculation and its numerical basis (2000). In: Proc. 10th International Congress of the International Radiation Protection Association IRPA, pp. 1–9. Hiroshima, Japan (May 2000). Paper T-4-4.
- Schraube, H., Heinrich, W., Leuthold, G., Roesler, S., Schraube, G., 2002a. Collating of Data for the Determination of the Exposure of Aviation Personnel Due to Cosmic Radiation, Concluded by 21 Dec 2000, and Calculation of Radiation Fields at Air Craft Flight Altitude during the Period of Solar Maximum Activity by 15 Nov 2000. Joint Report to The Council of the Dublin Institute for Advanced Studies (DIAS), 2002.
- Schraube, H., Leuthold, G., Heinrich, W., Roesler, S., Mares, V., Schraube, G., 2002b. EPCARD – European Program Package for the Calculation of Aviation Route Doses, User’s Manual, 2002. GSF-National Research Center, Neuherberg, Germany. ISSN 0721 - 1694. GSF-Report 08/02.
- Silari, M., Pozzi, F., 2017. The CERN-EU high-energy Reference Field (CERF) facility: applications and latest developments. EPJ Web Conf. 153, 03001 <https://doi.org/10.1051/epjconf/201715303>.
- Tagziria, H., Tanner, R.J., Bartlett, D.T., Thomas, D.J., 2004. Evaluation and Monte Carlo modelling of the response function of the Leake neutron area survey instrument. *Nucl. Instrum. Methods Phys. Res. Sect. A Accel. Spectrom. Detect. Assoc. Equip.* 531 (3), 596–606. <https://doi.org/10.1016/j.nima.2004.05.086>.
- Tobiska, W.K., Atwell, W., Beck, P., Benton, E., Copeland, K., Dyer, C., Gersey, B., Getley, I., Hands, A., Holland, M., Hong, S., Hwang, J., Jones, B., Malone, K., Meier, M.M., Mertens, C., Phillips, T., Ryden, K., Schwadron, N., Wender, S.A., Wilkins, R., Xapsos, M.A., 2015. Advances in atmospheric radiation measurements and modeling needed to improve air safety. *Space Weather* 13, 202–210. <https://doi.org/10.1002/2015SW001169>.
- Tromprier, F., Delacroix, S., Vabre, I., Jousard, F., Proust, J., 2007. Secondary exposure for 73 and 200 MeV proton therapy. *Radiat. Protect. Dosim.* 125 (1–4), 349–354. <https://doi.org/10.1093/rpd/ncm154>.
- Turecek, D., Jakubek, J., 2015. PIXET Software Package Tool for Control, Readout and Online Display Ofpixel Detectors Medipix/Timepix. Advacam, Prague.
- Uchihori, Y., Kitamura, H., Fujitaka, K., Dachev, T.P., Tomov, B.T., Dimitrov, P.G., Matviichuk, Y., 2002. Analysis of the calibration results obtained with Liulin-4J spectrometer–dosimeter on protons and heavy ions. *Radiat. Meas.* 35, 127–134. [https://doi.org/10.1016/S1350-4487\(01\)00286-4](https://doi.org/10.1016/S1350-4487(01)00286-4).
- Volnhals, M., 2012. Improvement of the HMGU Neutron Dosimeter by Monte Carlo Simulations and Measurements. Diploma Thesis, TU Munich.
- Wielunski, M., Schutz, R., Fantuzzi, E., Pagnamenta, A., Wahl, W., Palfalvi, J., Zombori, P., Andras, A., Stadtmann, H., Schmitzer, C., 2004. Study of the sensitivity of neutron sensors consisting of a converter plus Si charged-particle detector. *Nucl. Instrum. Methods A* 517, 240–253. <https://doi.org/10.1016/j.nima.2003.07.032>.
- Wielunski, M., Brall, T., Dommert, M., Trinkl, S., Rühm, W., Mares, V., 2018. Electronic neutron dosimeter in high-energy neutron fields. *Radiat. Meas.* 114, 12–18. <https://doi.org/10.1016/j.radmeas.2018.04.015>.
- Wissmann, F., Klages, T., 2018. A simple method to monitor the dose rate of secondary cosmic radiation at altitude. *J. Radiol. Prot.* 39, 71–84. <https://doi.org/10.1088/1361-6498/aaeae>.
- Yasuda, H., Yajima, K., 2018. Verification of cosmic neutron doses in long-haul flights from Japan. *Radiat. Meas.* 119, 6–11. <https://doi.org/10.1016/j.radmeas.2018.08.016>.
- Yasuda, H., Yajima, K., Sato, T., 2020. Investigation of using a long-life electronic personal dosimeter for monitoring aviation doses of frequent flyers. Available online 20 March 2020 *Radiat. Meas.* 106309. <https://doi.org/10.1016/j.radmeas.2020.106309> (in press).
- Zielczynski, M., Golnik, N., 1994. Recombination index of radiation quality - measuring and applications. *Radiat. Protect. Dosim.* 52 (1–4), 419–422. <https://doi.org/10.1093/oxfordjournals.rpd.a082226>.
- Zielczyński, M., Golnik, N., Gryziński, M.A., 2008. Applications of recombination chambers in the dosimetry of high energy radiation fields. *NUKLEONIKA* 53 (Suppl. 1), S45–S52.